

Hybrids of Silica/Poly(caprolactone coglycidoxypropyl trimethoxysilane) as Biomaterials

Tian Sang,[†] Siwei Li,[†] Hung-Kai Ting,[†] Molly M. Stevens,^{†,‡,§} C. Remzi Becer,[¶] and Julian R. Jones^{*,†}

[†]Department of Materials, Imperial College London, SW7 2AZ London, U.K.

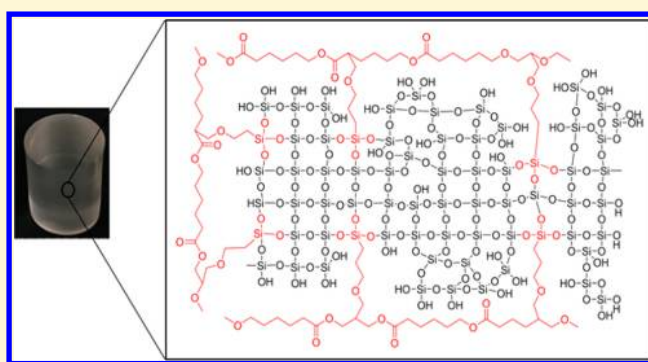
[‡]Institute of Biomedical Engineering, Imperial College London, SW7 2AZ London, U.K.

[§]Department of Bioengineering, Imperial College London, SW7 2AZ London, U.K.

[¶]Polymer Chemistry Laboratory, School of Engineering and Materials Science, Queen Mary, University of London, E1 4NS London, U.K.

Supporting Information

ABSTRACT: Bioactive glasses stimulate bone regeneration but are brittle. Biomaterials are needed that share load with bone, promote bone regeneration, and biodegrade at controlled rates. Sol–gel hybrids can achieve this through their intimate inorganic and organic conetworks, depending on the organic polymer used. Polycaprolactone degrades slowly but lacks functional groups for the critical step of covalent coupling to the silica conetwork. Here, we synthesized a novel copolymer of caprolactone and glycidoxypropyl trimethoxysilane through one-pot ring opening polymerization (ROP). Hybrids with different organic content were fabricated using such a copolymer for the first time. The copolymer can directly bond to a silica network due its trimethoxysilane groups, which can hydrolyze, leaving silanol groups that undergo polycondensation with silanol groups of the silica network. The number of repeating units of caprolactone and glycidoxypropyl trimethoxysilane functional groups were controlled via ROP. The mechanical properties of the hybrids were tuned by weight percent and the number of repeating units of caprolactone independently, producing a homogeneous material with high strength (64 MPa) and strain to failure (20%) that deformed in a unique linear elastic manner until failure. MC3T3-E1 preosteoblast cells adhered to the hybrids. Introducing such a copolymer created a new way to fabricate covalently bonded polycaprolactone/silica hybrids for future bone repair.



INTRODUCTION

Bone is the second most transplanted tissue.¹ It can heal itself if a defect is small and is continuously being remodelled by cells, partly as a response to mechanical stimuli.^{1–3} Current clinical bone regeneration approaches include bone grafting after trauma, tumor removal, or distraction osteogenesis.⁴ Surgeons tend to prefer autograft (transplanting bone from another site of the patient’s skeleton) over synthetic grafts, but this involves multiple operations, creation of another bone defect and increased risk of introducing postoperation infection.⁵ Synthetic biodegradable bone graft materials are available^{6–8} but tend to be bioactive glasses (BGs), ceramics, or mixtures of these with demineralized bone matrix.⁹

BG bonds to bone, stimulates bone regeneration, and is biodegradable.^{6,9,10} Its ability to provoke faster bone repair than other ceramic-based bone graft materials^{6,11–13} was attributed to its dissolution products stimulating cells.^{14–18} Bioglass clinical products (in powder form) have been used on more than a million patients.⁹ Bioactive glass can be made into porous scaffolds with compressive strength close to that of porous bone, but their brittleness limits their use to nonload

bearing indications.⁹ New devices are needed that can regenerate bone defects in cyclic loading sites.^{19–21} Composites can be made of bioactive glass particles within a biodegradable matrix,^{22,23} but the glass is likely to be covered by the polymer matrix, and matching the degradation rate of the two components is difficult.

Such problems can potentially be overcome through sol–gel hybrids with conetworks of organic polymers and inorganic silica. Class II hybrids have covalent bonds between the components.^{6,24–26} The organic network in the hybrids should be biodegradable, compatible with the sol–gel process, and have the ability to bond with the silica.⁶ Polycaprolactone (PCL) is one of the most popular biodegradable polymers due its superior rheological, viscoelastic properties and slow degradation rate, compared to other polyesters.^{3,27–30} Most previous studies incorporated PCL into the silica network by functionalizing commercially available PCL-diol with an

Received: February 20, 2018

Revised: May 16, 2018

Published: May 18, 2018

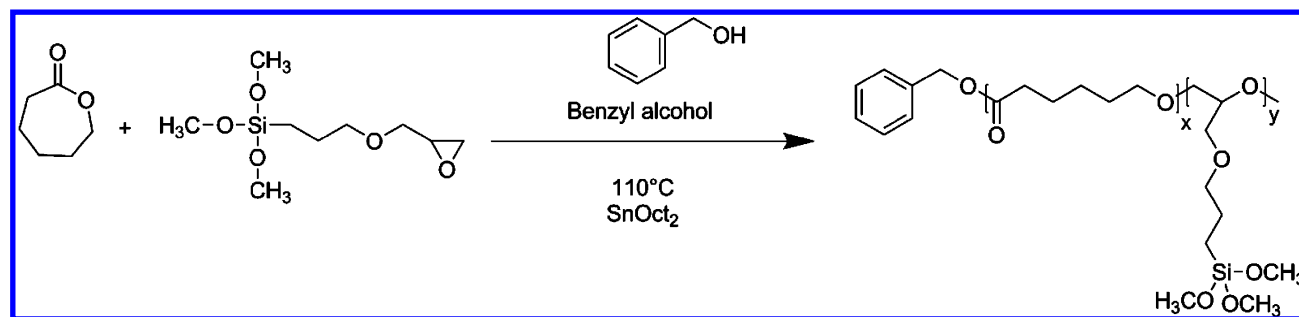


Figure 1. Ring opening polymerization of caprolactone and (3-glycidyloxypropyl) trimethoxysilane monomer, forming poly(CL-co-GPTMS) random copolymer.

organosilane coupling agent, for example 3-(triethoxysilyl)propyl isocyanate (ICPTS) or 3-glycidyloxypropyl trimethoxysilane (GPTMS),^{25,31} prior to its introduction into the sol-gel process. The aim was to form chemical bonds between Si-OH of the silica network and the hydrolyzed silanes of the functionalized PCL.^{25,32–34}

Using GPTMS coupling requires appropriate functional groups; the PCL-diol reaction with GPTMS is difficult to control, with low efficiency, resulting in poor mechanical properties, and ICPTS is a dangerous reagent.^{31,34,35} Promoting reaction between epoxide rings of GPTMS and the hydroxyl groups of PCL-diol is challenging due to the nucleophilic ability of the -OH group being low³⁶ and the number of coupling agents that can be attached per PCL-diol molecule restricted to two (the number of terminated hydroxyl groups).^{37,38} The majority of PCL/silica class II hybrids used ICPTS.^{25,31,34,37–40} It is not possible to vary molecular weight (MW) of the polymer and number of coupling agents per molecule independently when using PCL-diol and a coupling agent because the coupling occurs at the ends of the chain.

Here, we report the first class II hybrids made using a novel PCL-GPTMS copolymer prepared by one-pot ring-opening polymerization (ROP). Such copolymerization process allows control over the ratio of silane containing groups (from GPTMS) and caprolactone (CL) repeating units along the polymer chain. The aims of this study were to synthesize uniform class II hybrids using the new copolymer, determining the effect of organic content and the ratio of CL to silane containing units on mechanical properties and on the interactions of cells to the hybrids.

EXPERIMENTAL SECTION

Batch 1 hybrids were made with different organic weight percentages using the same copolymer, and batch 2 and 3 hybrids were made with different number of repeating units of CL while the amount of GPTMS and the organic weight percentage was kept constant.

Materials. ϵ -Caprolactone (CL, 97%), (3-glycidyloxypropyl) trimethoxysilane (GPTMS, $\geq 98\%$), benzyl alcohol (99.8%), tin(II) 2-ethylhexanoate (SnOct₂, 97%), tetraethyl orthosilicate (TEOS, 98%), calcium hydride (CaH₂, 99%), tetrahydrofuran (THF, $\geq 99.9\%$), chloroform-d (CDCl₃, 100%), methanol (99.8%), and hydrochloric acid (HCl, 1 M) were all purchased from Sigma-Aldrich (UK). Before polymerization, CL was purified by stirring over CaH₂ for 12 h prior to vacuum distillation to remove traces of water. Glassware was dried at 110 °C before use. MC3T3-E1 preosteoblast cell line was purchased from ATCC UK, and other cell reagents were purchased from Invitrogen and Sigma-Aldrich UK. The cell line was monolayer cultured in basal α -MEM with fetal calf serum (FCS, 10% v/v), streptomycin (100 μ g/mL), and penicillin (100 unit/mL). The cell culture environment was kept at 37 °C, 21% oxygen, and 5% carbon dioxide.

Poly(CL-co-GPTMS) Copolymer Synthesis. The polymer was synthesized using one-pot ROP, as shown in Figure 1. Prior to polymerization, a Schlenk tube was degassed under vacuum for 4 h to remove any moisture and filled with argon. CL, GPTMS, SnOct₂, and benzyl alcohol were first weighed according to the molar ratio in Table 1 and transferred by syringes (purged with argon) into the Schlenk

Table 1. Molecular Weight Characterization of Copolymers^a

polymer code	DP (CL:GPTMS)	$M_{n,Theo}$ (g/mol)	$M_{n,GPC}$ (g/mol)	PDI
P1	35:2	4594	3950	1.62
P2a	10:2	1744	1410	1.91
P2b	20:2	2884	2200	1.87
P2c	30:2	4024	3100	2.08
P2d	40:2	5164	4600	1.67
P2e	50:2	6304	6330	1.56
P2f	100:2	12 004	9130	1.92
P2g	200:2	23 404	19 540	2.17

^a M_n = number average molecular weight; PDI = polydispersity.

tube filled with argon. The mixed solution was further purged using argon gas for 1 h. The Schlenk tube was then placed in an oil bath at 110 °C for 24 h. Then, the copolymers were dissolved in tetrahydrofuran (THF) and precipitated in cold methanol to remove unreacted chemicals. Afterward, the copolymers were kept in vacuum at 40 °C to remove solvents before the next step.

Polymer Characterization. A 400 MHz Advance Bruker Proton nuclear magnetic resonance spectrometer (¹H NMR) was applied to investigate the polymer composition. For all polymers tested by NMR, the methylene peak (5.11 ppm) from benzyl alcohol was used as the internal standard because the molar ratio of benzyl alcohol was kept constant as an initiator. The monomer conversions were calculated by comparing the methylene peak at 5.11 ppm to the unreacted CL monomer peak at 4.23 ppm and unreacted GPTMS peak at 3.55 ppm. Number-average molecular weight (M_n) and polydispersity (P_d) for all polymers were determined by Agilent 1260 gel permeation chromatography (GPC), which was operated in THF with TEA (2% v/v) and equipped with two PLgel 5 μ m mixed-C columns (300 \times 7.5 mm), a PLgel 5 mm guard column (50 \times 7.5 mm), an auto sampler, a refractive index detector, and a variable wavelength detector. Prior to being injected to the GPC, all polymers were dissolved in THF and filtered through Nylon-6,6 filters with 0.2 μ m pore size. The calibration was based on PMMA standards in the range of 550–46 890 g/mol.

Hybrid Synthesis. Three batches of hybrids were synthesized (Table 2). The first batch included targeted organic polymer content from 50 to 100 wt % using the same copolymer of 35 CL units to 2 GPTMS molecules (35CL + 2GPTMS). The second and third batches included hybrids with constant 60 and 70 wt % organic component, respectively, to investigate the effect of changing the number of GPTMS units, using copolymers of 10 to 200 repeating units of CL and 2 GPTMS units.

Table 2. Mechanical Properties of the Poly(CL-co-GPTMS)/Silica Hybrids Tested in Compression^a

hybrid code	polymer code	org. target (wt %)	TGA org. (wt %)	ϵ_{\max} (%)	σ_{\max} (MPa)	E (MPa)
H1a	P1	50	49	7.1 ± 1	31 ± 2	452 ± 33
H1b	P1	60	58	7.3 ± 2	26 ± 6	377 ± 17
H1c	P1	70	70	9.8 ± 2	20 ± 5	285 ± 58
H1d	P1	80	82	17 ± 3	5 ± 2	36 ± 10
H1e	P1	100	90	24 ± 5	3 ± 2	13 ± 8
H2a	P2a	60	60	5.2 ± 1	7.8 ± 2	133 ± 15
H2b	P2b	60	58	5.7 ± 1	8.3 ± 1	166 ± 59
H2c	P2c	60	61	5.4 ± 1	10 ± 3	216 ± 27
H2d	P2d	60	58	7.3 ± 1	26 ± 3	255 ± 30
H2e	P2e	60	62	7.2 ± 1	17 ± 3	294 ± 41
H2g	P2f	60	59	7.1 ± 2	32 ± 1	471 ± 63
H2f	P2g	60	60	8.9 ± 1	53 ± 3	606 ± 82
H3a	P2e	70	69	12 ± 1	21 ± 2	192 ± 33
H3b	P2f	70	70	15 ± 1	35 ± 2	231 ± 10
H3c	P2g	70	70	20 ± 2	64 ± 3	317 ± 15

^aEach hybrid was synthesized with the corresponding polymer with a code that can be found in Table 1. ϵ_{\max} = strain at failure, σ_{\max} (failure stress), E = compression modulus.

The first step of synthesizing the hybrids was to dissolve the purified copolymer in THF. Then, TEOS was hydrolyzed with molar ratio TEOS:water:HCL = 1:4:0.015 in pot 2. Both pots were stirred vigorously for 40 min before mixing the two pots together.

The final mixture was further stirred for 30 min followed by transfer to three-column Teflon molds. The molds were sealed and placed into a 40 °C oven to gel and were aged for 20 days. The 20 day period was chosen to ensure the completion of conetwork formation and shrinkage. Gelation occurred after one week (the sol became solid, i.e. did not move if the mold was tipped). From weeks 1–2, condensation polymerization continued, and the gel shrank. No further shrinkage was observed after two weeks of aging. The molds were then opened in the oven for drying for another 10 days. At least three samples of each composition were made, and examples are shown in Figure 2.

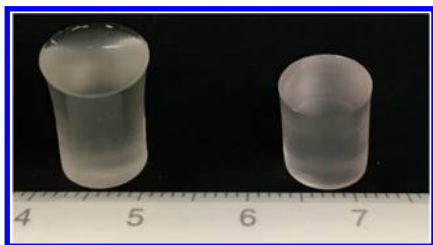


Figure 2. Examples of hybrids made (30 wt % inorganic content, polymer content included 35 repeating unit of CL and 2 repeating units of GPTMS). Scale is cm.

Hybrid Characterization. Hybrids were characterized using a Nicolet IS10 Fourier transform infrared spectrometer (FTIR, Thermo Scientific UK). An absorbance module with 32 scans was used. Uniaxial compression and cyclic loading tests on hybrids were performed using Zwick 1474 with a 100 kN load cell at 0.1 mm/min compression speed, following the ISO 640:2003 standard^{41,42} on crack-free cylinders of height to diameter ratio between 1 and 1.7. The weight percentages of inorganic and organic contents in the hybrids were measured by thermogravimetric analysis (TGA); samples were placed in a platinum crucible and ran by Netzsch sta 449c software from room temperature to 800 °C at 10 °C/min in air.

Cytotoxicity Test. MC3T3-E1 cells were used to perform in vitro cytotoxicity tests on the batch 2 hybrids in accordance with ISO10993-

5 and ISO10993-12 (biological evaluation of medical devices). Dissolution products from the hybrid samples (0.2 g/mL) were prepared in α -MEM at 37 °C for 72 h followed by filter sterilization. They were then diluted into 100, 75, 50, and 25% concentration and supplemented with 10% FCS prior to the tests. Medical grade polyethylene (PE) was noncytotoxic and used as the negative control. Polyurethane (PU) containing 0.1% (w/w) zinc diethyldithiocarbamate has cytotoxic response and was used as a positive control. Metabolically active cells convert MTT (3-(4,5-dimethylthiazol-2-yl)-2,5-diphenyltetrazolium bromide) into formazan, and such conversion was used to assess cell viability as a colorimetric assay. MC3T3-E1 cells were first cultured in α -MEM basal solution on plates (96 wells with 104 cells per well) and left for 24 h. The culture media was then removed, and the MC3T3-E1 cells were treated with the dissolution products from each hybrid sample as well as controls described above for 24 h. Then, the culture media was removed and followed by adding 50 μ L/well MTT solution (serum free α -MEM, 1 mg/mL). After 2 h incubation time, MTT was removed, and 100 μ L of isopropanol was added to each well. A Spectramax M5 microplate reader was used to measure the optical density at 570 nm when the formazan derivatives were fully dissolved.

Cell Culture on Hybrid Disks and Immunohistochemistry Staining. Hybrid samples were first sterilized (70% ethanol) for 1 min. Cultured MC3T3-E1 cells were harvested and left in basal α -MEM solution (106 cells/mL). The samples were washed with PBS before cell seeding. Ten microliters of the prepared cell suspension was seeded on each hybrid disc and incubated for 2 h at 37 °C, 5% CO₂, and 21% O₂. The cell-seeded samples were then immersed in basal α -MEM for another 72 h for cell culturing. Prior to immunohistochemical analysis, 4% (w/v) paraformaldehyde (PFA) was added to fix the cells after media removal and washing in PBS. Triton X-100 (0.5% (c/v)) in PBS containing 300 mM sucrose, 50 mM NaCl, 3 mM MgCl₂, and 20 mM HEPES at pH 7.2 was added to permeabilize the cell membranes. This was followed by blocking with 10 mg/mL BSA in PBS. Hybrid samples were incubated with anti-Vimentin antisera (1:500 dilution 10 mg/mL BSA in PBS) at 4 °C for 1 h, followed by hour-long incubation with Alexa Fluor 488-conjugated secondary antibody. F-actin was labeled following the instruction of CytoPainter F-actin staining kit (Abcam), and all samples were stained with DAPI nuclei staining (0.1 μ g/mL in PBS). Confocal microscopy (Leica SP5MP laser scanning confocal microscope) was applied to image the stained samples. Negative controls (omission of the primary antisera) were also performed with no staining observed.

RESULTS AND DISCUSSION

Polymer Characterization. Figure 3 shows ¹H NMR spectra of p(CL-co-GPTMS) and CL and GTPMS. The ¹H NMR spectrum of p(CL-co-GPTMS) contained all the peaks

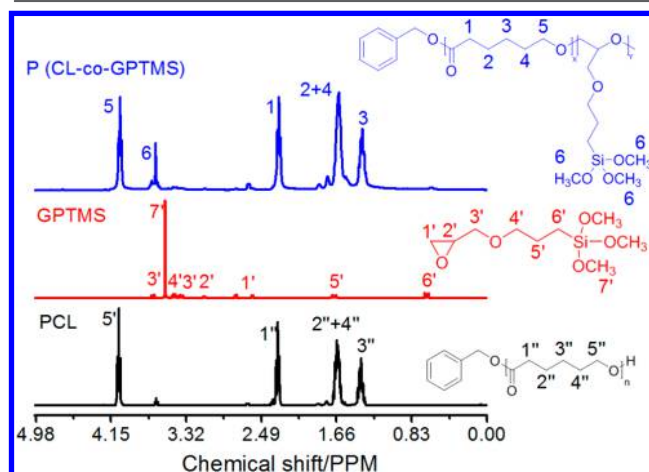


Figure 3. ¹H NMR spectra of PCL, GPTMS, and P(CL-co-GPTMS).

from pure PCL and peaks from GPTMS units. In the GPTMS spectrum, singlet peak 7' indicated by the hydrogens in Si–O–CH₃ is the most representative peak for GPTMS and the PCL in spectrum does not show this singlet peak. In the p(CL-co-GPTMS) spectrum, it appeared as singlet peak 6, proving that the GPTMS units successfully attached to PCL.

GPC traces of all p(CL-co-GPTMS) polymers made of different numbers of CL repeating units (10–200) and 2 units of GPTMS, are shown in Figure 4. The peak positions and their associated molar weights were close to the target values, as shown in Table 1.

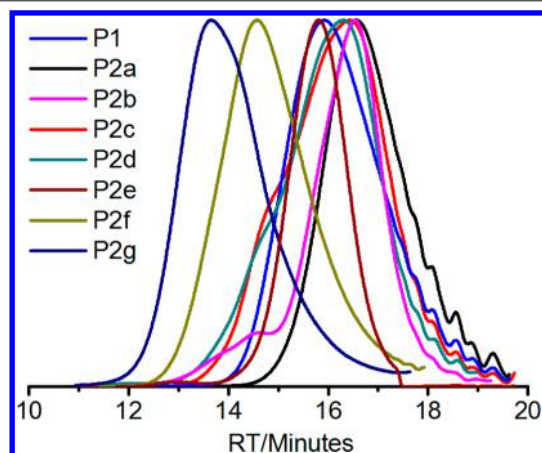


Figure 4. GPC traces of copolymers made of 10–200 repeating units of CL and 2 units of GPTMS.

Hybrid Characterization. Figure 2 shows photographs of transparent hybrid monoliths. Identification of organic polymer and inorganic silica network within the hybrids made of 50–100 wt % organic content were tested by FTIR (Figure S1). All hybrids gave vibration bands at 1725 and 2950 cm⁻¹, indicating C=O stretching and C–H stretching, respectively, of PCL. O–H stretching bands from both inorganic and organic parts were found at 3500 cm⁻¹. Si–C stretching bands were found at 780 cm⁻¹ due to the presence of GPTMS units within the polymer. Strong O–Si–O symmetric stretching and Si–OH stretching were also found at 1050 and 950 cm⁻¹, indicating a condensed silica network from the TEOS.

TGA traces of hybrids made of 50–100 wt % polymer are shown in Figure 5. All TGA traces flattened after the decomposition of the organic content and the residual weight remaining corresponds to the inorganic part. Table 2 shows that the organic weight percentages determined from TGA were close to the target organic weight percentages, except for the sample made without TEOS. This is due to the incorporation of GPTMS units within the polymer chain, where the trimethoxysilane groups cross-linked with each other, resulting in the formation of small amount of inorganic silica network. The derivatives of the TGA traces for batch 1 hybrids (Figure S2) indicated all hybrids went through multiple decomposition stages. They have their first decomposition at the temperature range 100–200 °C, attributed to the evaporation of solvents, water, and trace of unreacted monomers within the hybrids. The second stage of decomposition occurred between 220 and 370 °C and was primarily due to the thermal decomposition of part of the polymer. This is because the presence of trimethoxysilane groups cross-linked the polymers to the silica network, and part

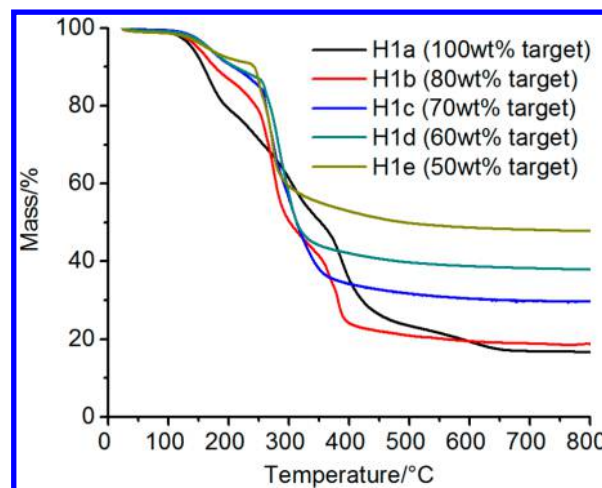


Figure 5. TGA traces of poly(CL-co-GPTMS)/silica hybrids made of 100 to 50 wt % targeted organic polymer contents.

of the polymers close to the trimethoxysilane groups show different thermal behavior from the rest, resulting in the polymer decomposing at different temperatures. Weight loss in the range 360 to 430 °C occurred only for hybrids with 80 wt % organic and 90 wt % organic, as this temperature range was close to the decomposition temperature of pure PCL.^{32,43} Because the two hybrids are made of mainly organic polymer contents, their thermal decompositions also show the transitions of pure PCL. Such multiple thermal decomposition was also found in other hybrid studies and copolymers of PCL.^{32,39,43–45}

Figure 6 shows the TGA traces of hybrids made of 60 wt % organic content, with the number of CL repeating units from

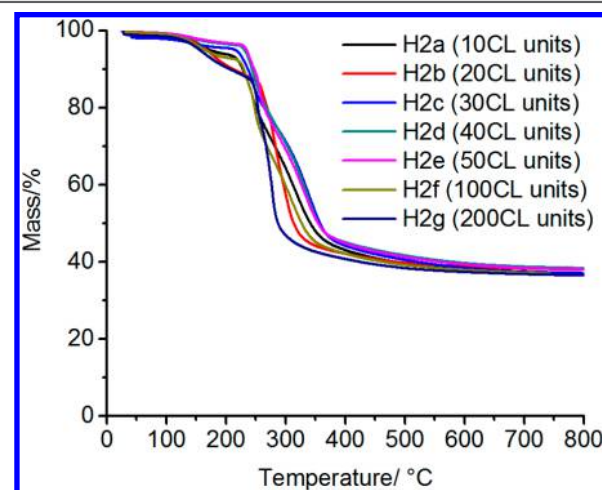


Figure 6. TGA traces of poly(CL-co-GPTMS)/silica hybrids made of 10–200 repeating units of CL with 60 wt % target organic content.

10 to 200. All hybrids obtained organic content close to the targeted 60 wt % with ± 1.4 wt % fluctuation. The result indicates the weight ratio can be precisely controlled with different molecular weights of the polymer.

Similar to batch 1 of the hybrids, the derivatives of TGA traces in Figure 6 (Figure S3) showed the first stage of decomposition from the evaporation of solvents, water, and unreacted monomers. As the number of repeating units of CL increased, peaks attributed to the decomposition of organic

polymer became broader (from ≈ 220 to ≈ 360 °C). The high temperature range within this stage (from ≈ 300 to ≈ 360 °C) have been seen in other PCL studies,³² whereas the lower temperature range (from ≈ 220 to ≈ 300 °C) could be caused by the incorporation of GPTMS groups that changed the partial orientation of molecular chains within the polymer, thus resulting in different thermal behaviors from pure PCL.

Figure 7 shows representative stress/strain curves of hybrids made with 50–90 wt % organic content using the same

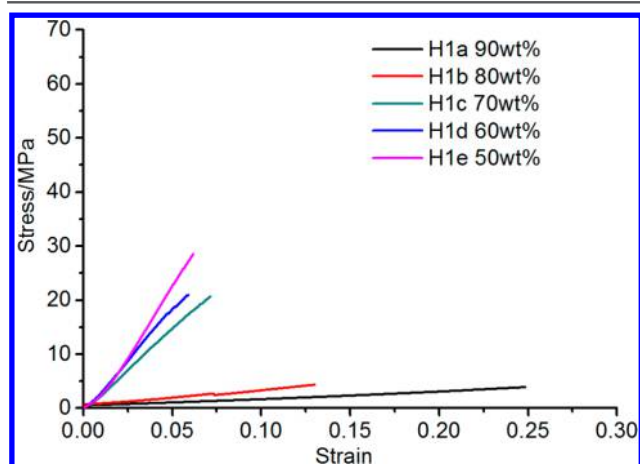


Figure 7. Uniaxial compression test curves for poly(CL-co-GPTMS)/silica hybrids with organic weight percentage from 90 to 50 wt %.

polymer (35 repeating units of CL and 2 units of GPTMS). As organic content increased from 50 to 90 wt %, the strain to failure increased from ≈ 7 to $\approx 24\%$, and hybrids became significantly less brittle. The stress–strain relationship appeared to remain linear elastic until failure. The bulk mechanical properties are shown in Table 2. The failure stress decreased from ≈ 30 to ≈ 3 MPa, and the compression modulus decreased from ≈ 500 to ≈ 13 MPa as organic content increased from 50 to 90 wt %, while strain to failure increased from 7 to 24%, indicating the hybrids become softer and more elastic as polymer content increased. Mechanical properties can therefore be tailored by changing the weight percentage of the polymer of the hybrids in a similar way to previous silica/PCL hybrids and composites.^{33,46,47} Allo et al. synthesized sol–gel derived PCL/bioactive glass hybrid materials using commercial PCL with 80 000 g/mol molecular weight.⁴⁷ They found the compression modulus decreased from ≈ 1388 to ≈ 552 MPa and strain at failure increased from 7.7 to 10.8% as the organic content increased from 10 to 60 wt %.⁴⁷ The new hybrids reported herein showed much more distinct changes in compressive mechanical properties and more strain to failure as the organic weight percentage increased. These findings could be due to the covalently bonded silica network and trimethoxysilane containing PCL.

Previous studies on glass/PCL hybrids have used commercial PCL^{31,33,46,47} and did not involve the investigation on the changes of compressive mechanical properties when the polymer length changes. Hybrids in Figure 8 were fabricated using polymers with 10–200 repeating units of CL and 2 GPTMS units. The weight percentage of the organic polymer content was constant at 60 wt % (H2a–H2g) and 70 wt % (H3a–H3c). Table 2 shows that at 60 wt % organic content the compression modulus increased from ≈ 140 to ≈ 611 MPa, maximum compression stress increased from ≈ 7 to ≈ 52 MPa,

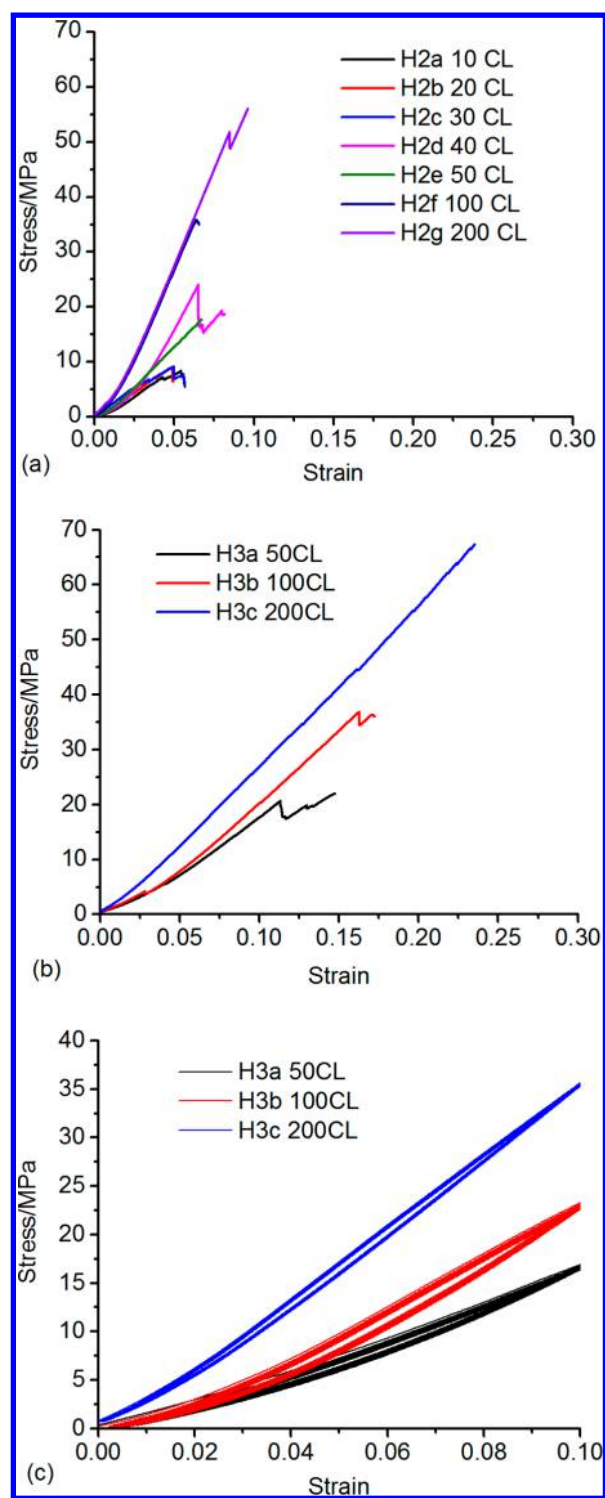


Figure 8. Uniaxial compression test curves for batch 2 and 3 poly(CL-co-GPTMS)/silica hybrids with 60 and 70 wt % organic content, respectively. (a) Polymers contain 10–200 caprolactone repeating units in H2a to H2g hybrids with 60 wt % organic content. (b) 50–200 caprolactone repeating units in H3a to H3c hybrids with 70 wt % organic content. (c) Cyclic compressions at strain 0 to 0.1 of H3a to H3c hybrids with 70 wt % organic content. Each cyclic compression has 10 repeating cycles.

and strain at failure increased from ≈ 5.5 to $\approx 8.5\%$ as the number of repeating units of CL in the polymer part increased from 10 to 200. Similar changes in compression mechanical

properties were also found in 70 wt % organic hybrids (H3a–H3c), suggesting the molecular weight of the polymer part plays an important role in altering the mechanical properties in the hybrids. The commercialized bone substitute HAPEX was a hydroxyapatite reinforced polyethylene composite with the formulation containing 40 vol % hydroxyapatite and often used to fix bone defects at nonload bearing sites.^{48–50} HAPEX has a Young's modulus ≈ 4.4 GPa at a strain to fracture $\approx 29\%$.⁵⁰ Cortical bone was found to have a compressive strength of ≈ 150 to 200 MPa and compressive modulus of 17–20 GPa^{51,52} when measured under similar conditions to those used herein. Trabecular bone has compressive strength between 2 and 10 MPa and modulus between 0.05 and 0.5 GPa.^{53,54} The mechanical properties of HAPEX were close to human bone, but it had a relatively small elastic region:^{50,55} HAPEX's yield stress (20–25 MPa) was much lower than its fracture stress (30–120 MPa),^{55,56} indicating that it is likely to undergo unrecoverable plastic deformation once 25 MPa of stress is exceeded.

Here, new hybrids, especially H3a–H3c (70 wt % organic), showed much greater elastic regions than the previous PCL–silica hybrids and HAPEX,^{47,55–59} making the new hybrids more capable of resisting permanent deformation at large strain (up to 20%). The yield strain of HAPEX in the elastic deformation region was not reported but can be estimated as $<4.5\%$ from published graphs.^{55,56,60} Cyclic loading in Figure 8c also proved that up to 10% strain, all three hybrids can return to their original shapes when the load was removed. They all have elastic properties with no obvious stress softening effects observed. Comparing with HAPEX, which is not biodegradable, and previous PCL–silica hybrids, such enlarged elastic property, and the fact they are biodegradable, makes the new hybrids possible to treat bone defects at load bearing sites.

Promoting cell attachment is an important quality for bone repair biomaterials. Out of the hybrids synthesized in this study, hybrids with 70 wt % organic polymer and ≥ 50 CL repeating units (H3a, H3b, and H3c) showed relatively high synthesis success (crack-free prior to any test) and impressive mechanical properties (Figure 8, Table 2); therefore, they were chosen to be examined for cytotoxicity level and osteogenic cell attachment. MTT assay was performed to test the cytotoxicity level using ISO 10993-12 standard wherein the 100% sample extract (undiluted) must have cell viability greater than 70% (in comparison to the noncytotoxic control) to be considered to have noncytotoxic effect, as was the case here. Cell viability of the 50% dilution of the sample extract must also be equal or greater than the undiluted extract. Figure 9 shows the viability of MC3T3 cells cultured in sample extracts and that all three hybrids passed the ISO 10993-12 standard. The hybrids made of polymer with 100 and 200 CL repeating units showed higher cell viability than the one made of 50 CL repeating units. The only difference in chemistry between 50 and 100 CL hybrids was increased GPTMS units on smaller CL chains. ¹H NMR found traces of CL-co-GPTMS polymer (polymer P) in the MEM cell media freeze-dried dissolution products of (50 CL) hybrid H3a only (Figure S5). It is possible that more small CL-GTPMS units are released from the 50 CL hybrids during extract preparation.

Immunohistochemistry was applied on the same hybrids after 72 h of cell culture. Confocal microscopy (Figure 10) shows the live MC3T3 cells spreading with vimentin (green), F-actin (red), intermediate filament proteins, and microfilaments. Cell spreading on a biomaterial is dependent on a

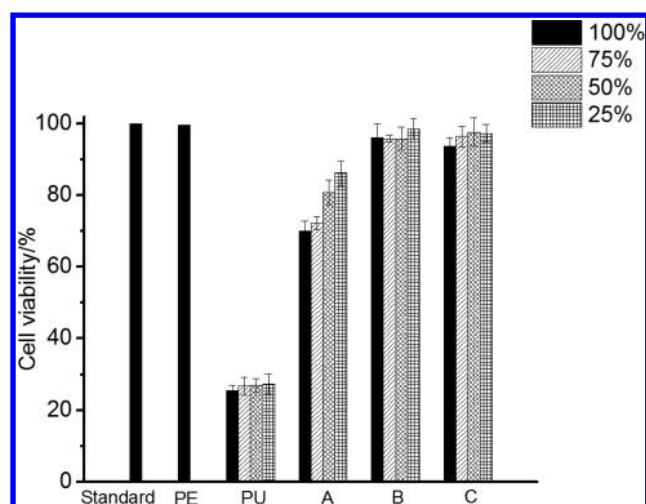


Figure 9. MC3T3 cell viability tests by MTT metabolic activity using ISO 10993 standards. Poly(CL-co-GPTMS)/silica hybrids were made of 70 wt % organic content with (A) 50 repeating units of CL, (B) 100 repeating units of CL, and (C) 200 repeating units of CL. Cell viabilities in 100% extract are 70.1% for (A), 95.97% for (B), and 93.65% for (C) compared to standard culture media and negative control (PE). Legend refers to the dilution of media exposed to the materials (extract), where 100% is undiluted. Error bars are \pm s.d., $n = 3$.

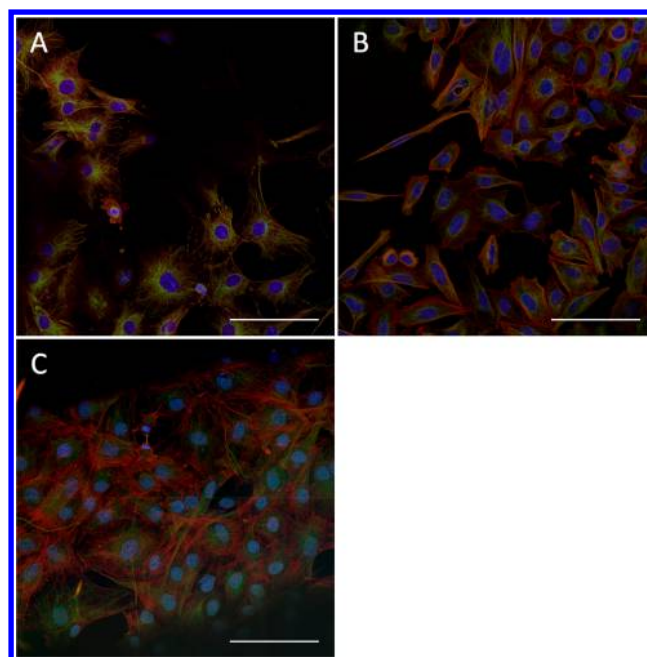


Figure 10. Confocal images of immunohistochemical staining of MC3T3 cells on poly(CL-co-GPTMS)/silica hybrids made with 60 wt % organic with (A) 50 repeating units CL, (B) 100 repeating units CL, and (C) 200 repeating units CL. Colors were associated with vimentin immunostain (green), f-actin labeling (red), and DAPI nuclear counterstain (blue). Scale bar = 100 μm .

number of factors. Moderately hydrophilic surfaces of suitable chemistry can support cell adhesion.^{61,62} Water contact angles on the hybrids featured in Figure 10 were similar, at between 84° to 93° . Figure 10 indicates cell attachment and spreading (evidenced by structure of staining act and vimentin proteins) was similar on each hybrid. However, there may have been slightly less spreading on 50 CL hybrids (Figure 10a), which

could be due to the hybrid's lower stiffness. Cell adhesions can be affected by the stiffness of biomaterials and the differences in stiffness between the material and the native tissue where the cells were derived.^{63,64} Pelham et al. found that 3T3 fibroblastic cells showed increased spreading on substrates made of the same material as with Young's modulus increased from 10 to 75 MPa,⁶⁵ with cell motility also decreasing ~40% as stiffness increased ~35%.⁶⁵ In-depth study regarding cellular response to our hybrid material will be conducted in further studies.

CONCLUSION

Class II poly(CL-co-GPTMS)-SiO₂ hybrids were successfully synthesized using different weight percentage of organic polymer and different number of repeating units of CL in the polymer. The mechanical properties of the hybrids can be tuned by changing the weight percentage and the length of the organic polymer in the hybrid. Hybrids made of 70 wt % organic polymer with 200 repeating units of CL per GPTMS unit had a compressive strength of 64 MPa at a strain of 20% and failed elastically. The hybrids also performed well under cyclic loads without hysteresis. They passed cytotoxicity tests according to ISO standards, and MC3T3 preosteoblast cells were able to adhere on the hybrid surfaces. The new poly(CL-co-GPTMS) copolymer allows a more efficient way to fabricate class II polycaprolactone-silica hybrids compared to functionalizing polycaprolactone, and they can be made with desired mechanical properties by controlling the total organic content, chain length, and spacing of covalent coupling to the inorganic component.

ASSOCIATED CONTENT

Supporting Information

The Supporting Information is available free of charge on the ACS Publications website at DOI: 10.1021/acs.chemmater.8b00751.

FTIR analysis of hybrids H1a–H1e; derivative of TGA traces of H1a–H1e and H2a–H2g; TGA traces of H3a–H3c hybrids; and ¹H NMR spectra of freeze-dried dissolution products of H3a–H3c hybrids in α-MEM (PDF)

AUTHOR INFORMATION

Corresponding Author

*E-mail: julian.r.jones@imperial.ac.uk.

ORCID

Molly M. Stevens: 0000-0002-7335-266X

C. Remzi Becer: 0000-0003-0968-6662

Julian R. Jones: 0000-0002-2647-8024

Author Contributions

The manuscript was written through contributions of all authors. H.-K.T. assisted with compression tests, and S.L. performed the cell studies on the hybrids. All authors have given approval to the final version of the manuscript.

Notes

The authors declare no competing financial interest.

ACKNOWLEDGMENTS

The authors would like to acknowledge financial support from the EPSRC (EP/M019950/1). Raw data can be obtained from rdm-enquiries@imperial.ac.uk.

REFERENCES

- (1) Dimitriou, R.; Jones, E.; McGonagle, D.; Giannoudis, P. Bone regeneration: current concepts and future directions. *BMC Med.* **2011**, *9*, 1–10.
- (2) Dimitriou, R.; Tsiridis, E.; Giannoudis, P. V. Current concepts of molecular aspects of bone healing. *Injury* **2005**, *36*, 1392–1404.
- (3) Jakus, A. E.; Rutz, A. L.; Jordan, S. W.; Kannan, A.; Mitchell, S. M.; Yun, C.; Koube, K. D.; Yoo, S. C.; Whiteley, H. E.; Richter, C.-P.; Galiano, R. D.; Hsu, W. K.; Stock, S. R.; Hsu, E. L.; Shah, R. N. Hyperelastic “bone”: A highly versatile, growth factor-free, osteo-generative, scalable, and surgically friendly biomaterial. *Sci. Transl. Med.* **2016**, *8*, 358ra127.
- (4) Aronson, J. Current concepts review - limb-lengthening, skeletal reconstruction, and bone transport with the Ilizarov method*. *J. Bone Jt. Surg* **1997**, *79*, 1243–1258.
- (5) Kubosch, E. J.; Bernstein, A.; Wolf, L.; Fretwurst, T.; Nelson, K.; Schmal, H. Clinical trial and in-vitro study comparing the efficacy of treating bony lesions with allografts versus synthetic or highly-processed xenogeneic bone grafts. *BMC Musculoskeletal Disord.* **2016**, *17*, 77.
- (6) Jones, J. R. Review of bioactive glass: From Hench to hybrids. *Acta Biomater.* **2013**, *9*, 4457–4486.
- (7) Macon, A. L. B.; Li, S.; Chung, J. J.; Nommeots-Nomm, A.; Solanki, A. K.; Stevens, M. M.; Jones, J. R. Ductile silica/methacrylate hybrids for bone regeneration. *J. Mater. Chem. B* **2016**, *4*, 6032–6042.
- (8) Valliant, E. M.; Jones, J. R. Softening bioactive glass for bone regeneration: sol-gel hybrid materials. *Soft Matter* **2011**, *7*, 5083–5095.
- (9) Jones, J. R.; Brauer, D. S.; Hupa, L.; Greenspan, D. C. Bioglass and bioactive glasses and their impact on healthcare. *Int. J. Appl. Glass Sci.* **2016**, *7*, 423–434.
- (10) Hench, L. L.; Splinter, R. J.; Allen, W. C.; Greenlee, T. K. Bonding mechanisms at the interface of ceramic prosthetic materials. *J. Biomed. Mater. Res.* **1971**, *5*, 117–141.
- (11) Oonishi, H.; Hench, L. L.; Wilson, J.; Sugihara, F.; Tsuji, E.; Kushitani, S.; Iwaki, H. Comparative bone growth behavior in granules of bioceramic materials of various sizes. *J. Biomed. Mater. Res.* **1999**, *44*, 31–43.
- (12) Oonishi, H.; Hench, L. L.; Wilson, J.; Sugihara, F.; Tsuji, E.; Matsuura, M.; Kin, S.; Yamamoto, T.; Mizokawa, S. Quantitative comparison of bone growth behavior in granules of Bioglass®, A-W glass-ceramic, and hydroxyapatite. *J. Biomed. Mater. Res.* **2000**, *51*, 37–46.
- (13) Oonishi, H.; Kushitani, S.; Yasukawa, E.; Iwaki, H.; Hench, L. L.; Wilson, J.; Tsuji, E.; Sugihara, T. Particulate Bioglass compared with hydroxyapatite as a bone graft substitute. *Clin. Orthop. Relat. Res.* **1997**, *334*, 316–325.
- (14) Hench, L. L.; Polak, J. M. Third-generation biomedical materials. *Science* **2002**, *295*, 1014–1017.
- (15) Hench, L. L.; Polak, J. M.; Xynos, I. D.; Buttery, L. D. K. Bioactive materials to control cell cycle. *Mater. Res. Innovations* **2000**, *3*, 313–323.
- (16) Xynos, I. D.; Edgar, A. J.; Buttery, L. D. K.; Hench, L. L.; Polak, J. M. Ionic products of Bioactive glass dissolution increase proliferation of human osteoblasts and induce insulin-like growth factor II mRNA expression and protein synthesis. *Biochem. Biophys. Res. Commun.* **2000**, *276*, 461–465.
- (17) Xynos, I. D.; Hukkanen, M. V. J.; Batten, J. J.; Buttery, L. D.; Hench, L. L.; Polak, J. M. Bioglass®45S5 stimulates osteoblast turnover and enhances bone formation in vitro: Implications and applications for bone tissue engineering. *Calcif. Tissue Int.* **2000**, *67*, 321–329.
- (18) Xynos, I. D.; Edgar, A. J.; Buttery, L. D. K.; Hench, L. L.; Polak, J. M. Gene-expression profiling of human osteoblasts following treatment with the ionic products of Bioglass® 45S5 dissolution. *J. Biomed. Mater. Res.* **2001**, *55*, 151–157.
- (19) Jones, J. R.; Ehrenfried, L. M.; Hench, L. L. Optimising bioactive glass scaffolds for bone tissue engineering. *Biomaterials* **2006**, *27*, 964–973.

- (20) Fu, Q.; Saiz, E.; Tomsia, A. P. Bioinspired strong and highly porous glass scaffolds. *Adv. Funct. Mater.* **2011**, *21*, 1058–1063.
- (21) Vallet-Regí, M.; Salinas, A.; Arcos, D. From the bioactive glasses to the star gels. *J. Mater. Sci.: Mater. Med.* **2006**, *17*, 1011–1017.
- (22) Dziadek, M.; Zagrajczuk, B.; Menaszek, E.; Cholewa-Kowalska, K. A new insight into in vitro behaviour of poly(ϵ -caprolactone)/bioactive glass composites in biologically related fluids. *J. Mater. Sci.* **2018**, *53*, 3939–3958.
- (23) Poh, P. S. P.; Huttmacher, D. W.; Holzapfel, B. M.; Solanki, A. K.; Stevens, M. M.; Woodruff, M. A. In vitro and in vivo bone formation potential of surface calcium phosphate-coated polycaprolactone and polycaprolactone/bioactive glass composite scaffolds. *Acta Biomater.* **2016**, *30*, 319–333.
- (24) Novak, B. M. Hybrid nanocomposite materials—between inorganic glasses and organic polymers. *Adv. Mater.* **1993**, *5*, 422–433.
- (25) Tian, D.; Dubois, P.; Jerome, R. A new poly(ϵ -caprolactone) containing hybrid ceramer prepared by the sol-gel process. *Polymer* **1996**, *37*, 3983–3987.
- (26) Sanchez, C.; Ribot, F.; Rozes, L.; Alonso, B. Design of Hybrid Organic-Inorganic Nanocomposites Synthesized Via Sol-Gel Chemistry. *Mol. Cryst. Liq. Cryst. Sci. Technol., Sect. A* **2000**, *354*, 143–158.
- (27) Woodruff, M. A.; Huttmacher, D. W. The return of a forgotten polymer—Polycaprolactone in the 21st century. *Prog. Polym. Sci.* **2010**, *35*, 1217–1256.
- (28) Labet, M.; Thielemans, W. Synthesis of polycaprolactone: a review. *Chem. Soc. Rev.* **2009**, *38*, 3484–3504.
- (29) Feiner, R.; Engel, L.; Fleischer, S.; Malki, M.; Gal, I.; Shapira, A.; Shacham-Diamand, Y.; Dvir, T. Engineered hybrid cardiac patches with multifunctional electronics for online monitoring and regulation of tissue function. *Nat. Mater.* **2016**, *15*, 679–685.
- (30) Hollister, S. J. Porous scaffold design for tissue engineering. *Nat. Mater.* **2005**, *4*, 518–524.
- (31) Rhee, S.-H.; Choi, J.-Y.; Kim, H.-M. Preparation of a bioactive and degradable poly(ϵ -caprolactone)/silica hybrid through a sol-gel method. *Biomaterials* **2002**, *23*, 4915–4921.
- (32) Allo, B. A.; Rizkalla, A. S.; Mequanint, K. Synthesis and electrospinning of ϵ -Polycaprolactone-Bioactive glass hybrid biomaterials via a sol-gel process. *Langmuir* **2010**, *26*, 18340–18348.
- (33) Rhee, S.-H. Effect of molecular weight of poly(ϵ -caprolactone) on interpenetrating network structure, apatite-forming ability, and degradability of poly(ϵ -caprolactone)/silica nano-hybrid materials. *Biomaterials* **2003**, *24*, 1721–1727.
- (34) Mondal, D.; Rizkalla, A. S.; Mequanint, K. Bioactive borophosphosilicate-polycaprolactone hybrid biomaterials via a non-aqueous sol gel process. *RSC Adv.* **2016**, *6*, 92824–92832.
- (35) Sachot, N.; Mateos-Timoneda, M. A.; Planell, J. A.; Velders, A. H.; Lewandowska, M.; Engel, E.; Castano, O. Towards 4th generation biomaterials: a covalent hybrid polymer-ormoglass architecture. *Nanoscale* **2015**, *7*, 15349–15361.
- (36) Gabrielli, L.; Connell, L.; Russo, L.; Jimenez-Barbero, J.; Nicotra, F.; Cipolla, L.; Jones, J. R. Exploring GPTMS reactivity against simple nucleophiles: chemistry beyond hybrid materials fabrication. *RSC Adv.* **2014**, *4*, 1841–1848.
- (37) Catauro, M.; Raucci, M. G.; de Gaetano, F.; Buri, A.; Marotta, A.; Ambrosio, L. Sol-gel synthesis, structure and bioactivity of Polycaprolactone/CaO • SiO₂ hybrid material. *J. Mater. Sci.: Mater. Med.* **2004**, *15*, 991–995.
- (38) Chen, J.; Que, W.; Xing, Y.; Lei, B. Molecular level-based bioactive glass-poly (caprolactone) hybrids monoliths with porous structure for bone tissue repair. *Ceram. Int.* **2015**, *41*, 3330–3334.
- (39) Lee, K. M.; Knight, P. T.; Chung, T.; Mather, P. T. Polycaprolactone-POSS chemical/physical double networks. *Macromolecules (Washington, DC, U. S.)* **2008**, *41*, 4730–4738.
- (40) Rhee, S.-H.; Lee, Y.-K.; Lim, B.-S.; Yoo, J. J.; Kim, H. J. Evaluation of a novel poly(ϵ -caprolactone)-organosiloxane hybrid material for the potential application as a bioactive and degradable bone substitute. *Biomacromolecules* **2004**, *5*, 1575–1579.
- (41) Chung, J. J.; Li, S.; Stevens, M. M.; Georgiou, T. K.; Jones, J. R. Tailoring mechanical properties of sol-gel hybrids for bone regeneration through polymer structure. *Chem. Mater.* **2016**, *28*, 6127–6135.
- (42) Poologasundarampillai, G.; Yu, B.; Tsigkou, O.; Wang, D.; Romer, F.; Bhakhri, V.; Giuliani, F.; Stevens, M. M.; McPhail, D. S.; Smith, M. E.; Hanna, J. V.; Jones, J. R. Poly(γ -glutamic acid)/silica hybrids with calcium incorporated in the silica network by use of a calcium alkoxide precursor. *Chem. - Eur. J.* **2014**, *20*, 8149–8160.
- (43) Wang, L.-s.; Cheng, S.-x.; Zhuo, R.-x. Syntheses and properties of novel copolymers of polycaprolactone and aliphatic polycarbonate based on ketal-protected dihydroxyacetone. *Polym. Bull.* **2014**, *71*, 47–56.
- (44) Chavalitpanya, K.; Phattananudee, S. Poly(lactic acid)/polycaprolactone blends compatibilized with block copolymer. *Energy Procedia* **2013**, *34*, 542–548.
- (45) Wu, C.-M.; Huang, C.-W. Melting and crystallization behavior of copolymer from cyclic butylene terephthalate and polycaprolactone. *Polym. Eng. Sci.* **2011**, *51*, 1004–1013.
- (46) Rhee, S.-H. Bone-like apatite-forming ability and mechanical properties of poly(ϵ -caprolactone)/silica hybrid as a function of poly(ϵ -caprolactone) content. *Biomaterials* **2004**, *25*, 1167–1175.
- (47) Allo, B. A.; Rizkalla, A. S.; Mequanint, K. Hydroxyapatite formation on sol-gel derived poly(ϵ -caprolactone)/Bioactive glass hybrid biomaterials. *ACS Appl. Mater. Interfaces* **2012**, *4*, 3148–3156.
- (48) Roeder, R. K.; Converse, G. L.; Kane, R. J.; Yue, W. Hydroxyapatite-reinforced polymer biocomposites for synthetic bone substitutes. *JOM* **2008**, *60*, 38–45.
- (49) Bonfield, W. Composites for bone replacement. *J. Biomed. Eng.* **1988**, *10*, 522–526.
- (50) Bonfield, W. Hydroxyapatite-Reinforced Polyethylene as an Analogous Material for Bone Replacement. *Ann. N. Y. Acad. Sci.* **1988**, *523*, 173–177.
- (51) Carter, D. R.; Hayes, W. C. Bone compressive strength: the influence of density and strain rate. *Science* **1976**, *194*, 1174–1176.
- (52) Mirzaali, M. J.; Schwiedrzik, J. J.; Thaiwichai, S.; Best, J. P.; Michler, J.; Zysset, P. K.; Wolfram, U. Mechanical properties of cortical bone and their relationships with age, gender, composition and microindentation properties in the elderly. *Bone (N. Y., NY, U. S.)* **2016**, *93*, 196–211.
- (53) Linde, F.; Hvid, I. Stiffness behaviour of trabecular bone specimens. *J. Biomech.* **1987**, *20*, 83–89.
- (54) Linde, F.; Hvid, I.; Jensen, N. C. Material Properties of Cancellous Bone in Repetitive Axial Loading. *Eng. Med.* **1985**, *14*, 173–177.
- (55) Wang, M.; Ladizesky, N. H.; Tanner, K. E.; Ward, I. M.; Bonfield, W. Hydrostatically extruded HAPEX. *J. Mater. Sci.* **2000**, *35*, 1023–1030.
- (56) Kang, X.; Zhang, W.; Yang, C. Mechanical properties study of micro- and nano-hydroxyapatite reinforced ultrahigh molecular weight polyethylene composites. *J. Appl. Polym. Sci.* **2016**, *133*, 42869.
- (57) Fiedler, T.; Videira, A. C.; Bártolo, P.; Strauch, M.; Murch, G. E.; Ferreira, J. M. F. On the mechanical properties of PLC-bioactive glass scaffolds fabricated via BioExtrusion. *Mater. Sci. Eng., C* **2015**, *57*, 288–293.
- (58) Ji, L.; Wang, W.; Jin, D.; Zhou, S.; Song, X. In vitro bioactivity and mechanical properties of bioactive glass nanoparticles/polycaprolactone composites. *Mater. Sci. Eng., C* **2015**, *46*, 1–9.
- (59) Williams, J. M.; Adewunmi, A.; Schek, R. M.; Flanagan, C. L.; Krebsbach, P. H.; Feinberg, S. E.; Hollister, S. J.; Das, S. Bone tissue engineering using polycaprolactone scaffolds fabricated via selective laser sintering. *Biomaterials* **2005**, *26*, 4817–4827.
- (60) Wang, M.; Bonfield, W. Chemically coupled hydroxyapatite-polyethylene composites: structure and properties. *Biomaterials* **2001**, *22*, 1311–1320.
- (61) Geckeler, K. E.; Wacker, R.; Aicher, W. K. Biocompatibility correlation of polymeric materials using human osteosarcoma cells. *Naturwissenschaften* **2000**, *87*, 351–354.
- (62) Chung, J. J.; Sum, B. S. T.; Li, S.; Stevens, M. M.; Georgiou, T. K.; Jones, J. R. Effect of Comonomers on Physical Properties and Cell

Attachment to Silica-Methacrylate/Acrylate Hybrids for Bone Substitution. *Macromol. Rapid Commun.* **2017**, *38*, 1700168.

(63) Khatiwala, C. B.; Peyton, S. R.; Metzke, M.; Putnam, A. J. The regulation of osteogenesis by ECM rigidity in MC3T3-E1 cells requires MAPK activation. *J. Cell. Physiol.* **2007**, *211*, 661–672.

(64) Engler, A. J.; Sen, S.; Sweeney, H. L.; Discher, D. E. Matrix Elasticity Directs Stem Cell Lineage Specification. *Cell* **2006**, *126*, 677–689.

(65) Pelham, R. J.; Wang, Y.-l. Cell locomotion and focal adhesions are regulated by substrate flexibility. *Proc. Natl. Acad. Sci. U. S. A.* **1997**, *94*, 13661–13665.